Sickel Konrad[1] Bubnik Vojtech[2],
[1]Pattern Recognition Lab, Department of Computer Science, Friedrich-Alexander-Universität Erlangen-Nürnberg, Martensstr. 3, 91058 Erlangen, Germany
[2]Siemens Hearing Instruments, Inc., 10 Constitution Ave, Piscataway, NJ 08855.

Iterative Closest Point Algorithm for Rigid Registration of Ear Impressions

Introduction

Registration of surface meshes is a fundamental task with numerous applications in different fields such as computer vision and medical imaging. The general registration task is defined by computing a transformation to align two or more surfaces.
The state-of-the-art solution is usually based on an iterative closest point (ICP) algorithm. The algorithm was independently introduced by Besl and McKay [2], Chen and Medioni [4] and Zhang [10]. Besl et al. used the point-to-point metric, while Chen and Medioni developed the point-to-plane metric. Zhang proposed an efficient rejection strategy of invalid point pairs. Since, the first introduction of the ICP, many different variations were proposed [8].
In this work, a two-step version using the point-to-point, the point-to-plane metric as well as an efficient surface reduction and point-matching technique is proposed. Our aim is to compute a fast, robust and accurate registration of ear impressions, see Figure 1.

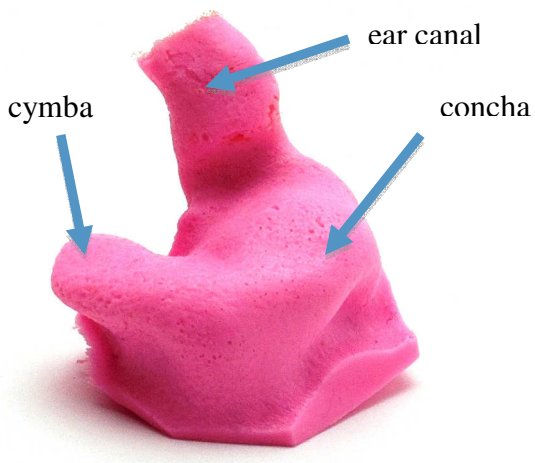

Fig. 1: Example of an ear impression. Please refer to [5] for a detailed explanation of key anatomical features.

An ear impression is acquired by placing a malleable material in the patient's ear. The settled material is scanned afterwards using a 3-D scanner. The resulting mesh is a smooth open 2-D manifold. However, often the meshes contain huge amounts of noise in the area of the deepest point of the ear canal and the outer ear. Some example meshes are depicted in Figure 2. The ear meshes are processed utilizing a computer-aided-design (CAD) system to model customized in-the-ear hearing aids, see Figure 3.
The goal of our work is to improve and speed up the preprocessing of the meshes in the CAD system. The CAD system as described in [9] utilizes anatomical important features detected on the meshes. Ear shapes show strong shape variations, the identification of features in a robust and reliable way is a complex task.

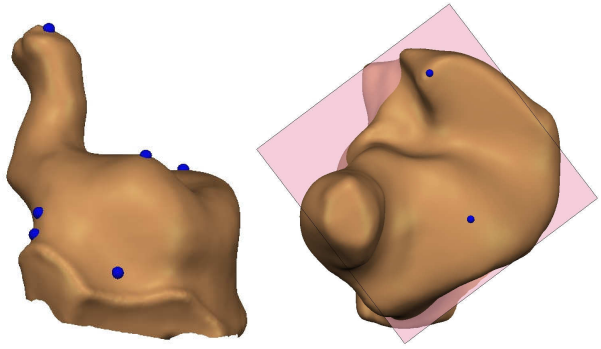

Fig. 2: Two examples of ear surfaces including a subset of anatomical important feature points shown as blue dots.

Similar work was done by Zouhar et al. [11] and Paulsen et al. [7]. The former registered left and right ear impressions using extracted anatomical feature points. The latter worked on the identification of a general ear shape based on features and mesh deformations.
The organization of the paper is as follows. In the next section, we discuss the applied methods. This is followed by a description of the carried out experiments and the corresponding results. Finally, we conclude and discuss the achieved results.

Fig. 3: In-the-ear hearing aids are typically build in three size categories: In-the-ear (ITE) devices (left), in-the-canal (ITC) devices (middle) and completely-in-the-canal (CIC) devices (right).

Material and Methods

The scanned ear impressions result in point clouds containing up to 30,000 vertices. To achieve a fast and robust registration of two of these meshes, we use two steps:

1. Reduction of the surface mesh to a so-called centerline. Applying an ICP with point-to-point metric to achieve a coarse registration.
2. Applying an ICP with point-to-plane metric on a sub sampled mesh to compute the final registration.

The centerline of an ear surface is computed similar to an active contour (snake) [6]. Therefore, we utilize one property of the data – the opening at the bottom of the surface. It allows the definition of a plane, which is used to slice the mesh equidistantly beginning at the canal tip of the mesh. The resulting closed contours, more precisely the contour centers construct the initial centerline. Afterwards the centerline is refined and improved by applying internal and external forces on the line as defined below:

A. Alexandrov, I. Fedorov, Y. Gulyaev, S. Shchukin, H. Feussner, R. Bauernschmitt, N. Navab, J. Hornegger, E.W. Mayr, S. Umnyshkin, S. Selishchev, I. Spiridonov, A. Nikolaev, V. Kutuzov, V. Shapovalov (Eds.): Proceedings of the 6-th Russian-Bavarian Conference on Bio-Medical Engineering, pp. 142 –145, 2010, ISBN: 978-5-7038-34-59-6

$$E_{\text{int}}(i) = l(i-1) + l(i+1) - 2l(i), \quad (1)$$

$$E_{ext}(i) = \frac{1}{N}\sum_{r=1}^{N}\frac{x_{r,i}}{|x_{r,i}|}, \quad (2)$$

$$l'(i) = l(i) + \alpha E_{\text{int}}(i) + \beta E_{ext}(i). \quad (3)$$

In eq. (2), $x_{r,i}$ denotes the hit point with the mesh of a random ray r emitted from the centerline point $l(i)$ and N is the number of rays. The final update rule of a centerline point $l(i)$ is a weighted combination of the internal and external force, where $\alpha = 0.04$ and $\beta = 1.0$. The centerline points are updated according to eq. (3) until convergence. An example for the initial and the refined centerline is given in Figure 4.

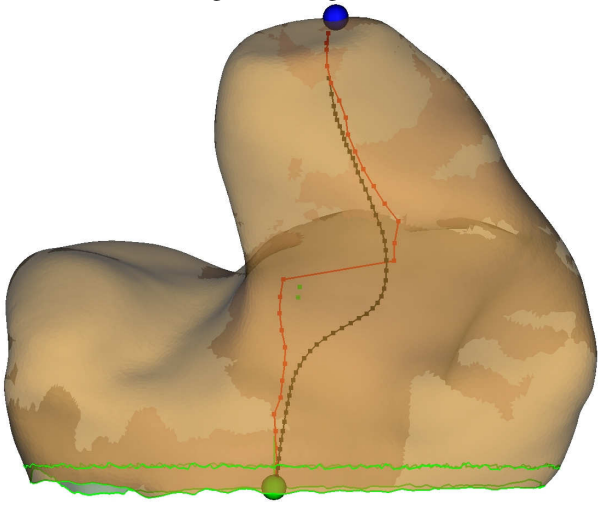

Fig. 4: Centerline of an ear impression. The initial centerline is colored in red and the refined centerline in black.

The centerlines are used in a preregistration step using the ICP algorithm. A critical step of the ICP is the matching of point pairs, which can be computational expensive. We use the fact that the centerlines are ordered from top to bottom for an efficient point matching technique. We shift the shorter centerline along the longer, adjust the size of the longer one and compute the point matches based on the point indexes. For every shift step, we compute the ICP and store the transformation matrix and the registration error. For the final registration only the best transformation matrices are kept.

To solve the ICP, we utilize the SVD-based strategy proposed by Arun et al. [1]. The basic optimization problem is formulated in eq. (4):

$$\varepsilon = \sum_{i=1}^{N}\left\|Rp_i + t - q_i\right\|^2, \quad (4)$$

where $q_i \in Q$ is the closed point to $p_i \in P$. In a first step, the translation is decoupled from the rotation by utilizing the center points of the point clouds.

$$\bar{p} = \frac{1}{N}\sum_{i=1}^{N} p_i, \qquad p'_i = p_i - \bar{p}$$

$$\bar{q} = \frac{1}{N}\sum_{i=1}^{N} q_i, \qquad q'_i = q_i - \bar{q}$$

$$\varepsilon = \sum_{i=1}^{N}\left\|Rp'_i - q'_i\right\|^2 \quad (5)$$

Using the translated point clouds P' and Q', we can build a matrix

$$H = \sum_{i=1}^{N} p'_i q'_i.$$

The application of the SVD yields $H = U\Sigma V^t$. $R = VU^t$ then gives the desired rotation matrix R. Afterwards the translation can be computed using

$$t = \bar{q} - R\bar{p}. \quad (6)$$

As result we obtain a vector of transformations, which can be used as starting point for the second ICP.

For the second ICP, we used the point-to-plane metric, in contrast to the point-to-point error metric; it utilizes the surface normal (n_i) information and allows that smooth or planar areas of the meshes slide over each other easily. Hence, the optimization problem is defined as

$$\varepsilon = \sum_{i=1}^{N}\left\|\left(Rp_i + t - q_i\right)n_i\right\|^2. \quad (7)$$

In eq. (7) q_i denotes a point on the tangent plane s_i [4]. Given that we have an initial alignment, we can linearize the problem by approximating $\cos\alpha = 1$ and $\sin\alpha = \alpha$, which allows the approximation of the rotation matrix R:

$$R = \begin{pmatrix} 1 & -\gamma & \beta \\ \gamma & 1 & -\alpha \\ -\beta & \alpha & 1 \end{pmatrix}. \quad (8)$$

Substitution of eq. (8) into (7) yields

$$\varepsilon = \sum_{i=1}^{N}\left[\left(p_i - q_i\right)n_i + tn_i + ra_i\right]^2, \quad (9)$$

where $a = p \times n$ and $r = (\alpha\ \beta\ \gamma)^t$. To minimize eq. (9), the partial derivatives can be used. The derivatives can be collected an expressed in matrix form (eq. (10)) allowing the representation of the optimization task as $Ax = b$. Eq. (10) can be solved using standard methods like Cholesky or LU-decomposition [11].

Results

For our experiments we acquired a sample set of 400 meshes. In order to compute an exact registration error we evaluated the registration a sample with itself. To simulate the real task the samples were modified. The modifications included a cutting of the mesh to remove approximately 25 percent of the mesh, a rotation about

$$\sum_{i=1}^{N}\begin{pmatrix} a_{i,x}a_{i,x} & a_{i,x}a_{i,y} & a_{i,x}a_{i,z} & a_{i,x}n_{i,x} & a_{i,x}n_{i,y} & a_{i,x}n_{i,z} \\ a_{i,y}a_{i,x} & a_{i,y}a_{i,y} & a_{i,y}a_{i,z} & a_{i,y}n_{i,x} & a_{i,y}n_{i,y} & a_{i,y}n_{i,z} \\ a_{i,z}a_{i,x} & a_{i,z}a_{i,y} & a_{i,z}a_{i,z} & a_{i,z}n_{i,x} & a_{i,z}n_{i,y} & a_{i,z}n_{i,z} \\ n_{i,x}a_{i,x} & n_{i,x}a_{i,y} & n_{i,x}a_{i,z} & n_{i,x}n_{i,x} & n_{i,x}n_{i,y} & n_{i,x}n_{i,z} \\ n_{i,y}a_{i,x} & n_{i,y}a_{i,y} & n_{i,y}a_{i,z} & n_{i,y}n_{i,x} & n_{i,y}n_{i,y} & n_{i,y}n_{i,z} \\ n_{i,z}a_{i,x} & n_{i,z}a_{i,y} & n_{i,z}a_{i,z} & n_{i,z}n_{i,x} & n_{i,z}n_{i,y} & n_{i,z}n_{i,z} \end{pmatrix}\begin{pmatrix} \alpha \\ \beta \\ \delta \\ t_x \\ t_y \\ t_z \end{pmatrix} = -\sum_{i=1}^{N}\begin{pmatrix} a_{i,x}(p_i - q_i)n_i \\ a_{i,y}(p_i - q_i)n_i \\ a_{i,z}(p_i - q_i)n_i \\ n_{i,x}(p_i - q_i)n_i \\ n_{i,y}(p_i - q_i)n_i \\ n_{i,z}(p_i - q_i)n_i \end{pmatrix}. \quad (10)$$

10 degrees followed by the application of random noise, see Figure 5.

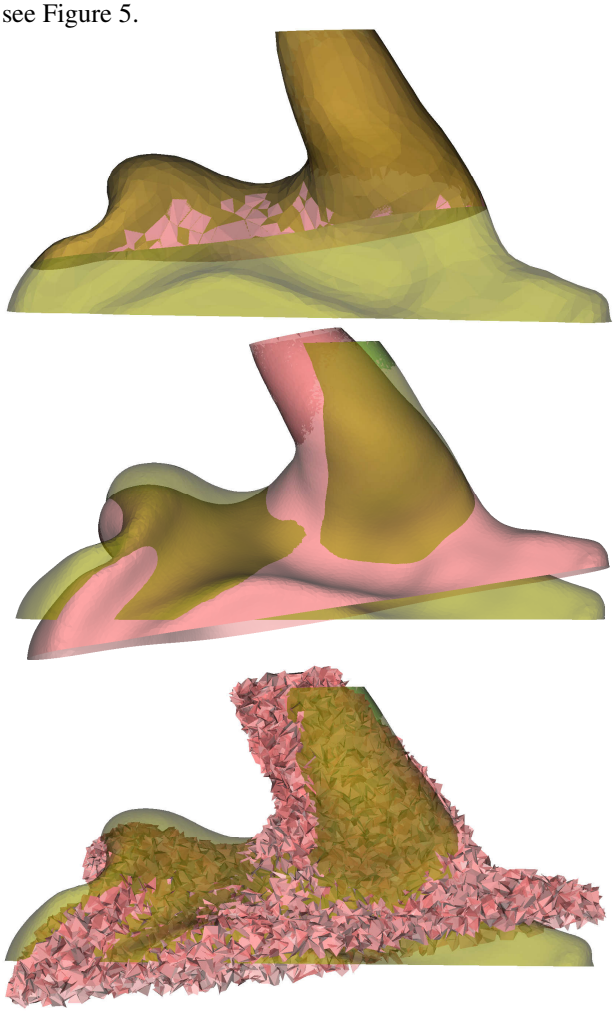

Fig. 5: Modified samples for the registration evaluation. The first picture shows a sample, which was cut at the bottom. In the middle the applied rotation is shown and at the bottom the rotation in combination with random noise is depicted.

In our experiments we focused on how to select points, how to reject point pairs and if weighting of point pairs is beneficial. If not denoted otherwise, we utilized 1000 point pairs, a two value threshold rejection technique and no point pair weighting. The registration error is defined as the average sum of squared distances between the modified samples (computed using the original sample).
We compared random and uniform point selection. As reference, we also computed the registration error for all points. The results are listed in Table 1 and visualized in Figure 6.

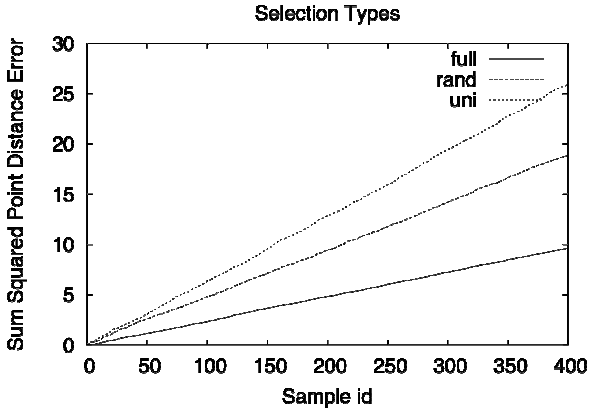

Fig. 6: Comparison of the cumulative registration error of the three selection techniques.

Point selection	Error	Time in sec
Full	0.0244	25.8
Random	0.0478	1.6
Uniform	0.0657	1.7

Tab. 2: Results of the different point selection strategies, showing the average registration error and the average computation time. Note: The computation time includes data loading and modification.

The results clearly indicate that the uniform selection of points is far worse than selection of random points. Naturally, selecting all points yields the best result. However, the random selection error is only slightly larger. In addition, the random selection is approximately 16 times faster.
To handle the implicit assumption of full overlap of the surfaces being registered and the theoretical assumption, that the points are exact rather than measured, a maximum matching threshold (d_{max}) is applied [8,10]. We compared five rejection strategies, including not using rejection at all. The simplest one is rejection of point-pairs based on a threshold value. We investigated two variations: one iteration with a medium threshold $d_{max} = 2$ and one iteration with a large threshold $d_{max} = 2.5$ followed by one with a small $d_{max} = 1.0$ threshold. Furthermore, we evaluated the rejection of the worst pairs and rejection based on the standard deviation of the point pair distance [8]. In the former we excluded the worst 10 percent and in the latter we excluded point-pairs with a distance greater than $d_{max} = 2.5\sigma$, where σ is

the standard deviation. The results are listed in Table 2 and visualized in Figure 7.

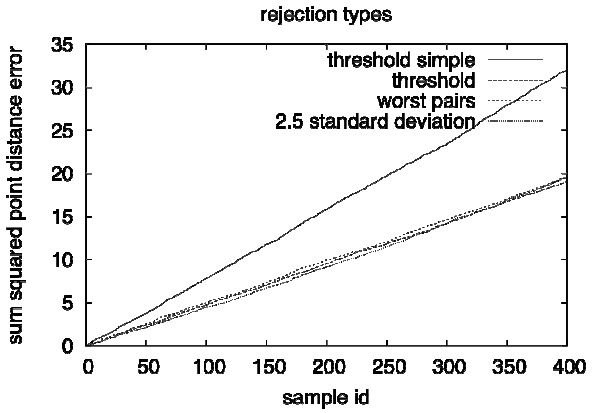

Fig. 7: Comparison of the cumulative registration error of the five rejection techniques (No rejection not shown).

Point pair rejection	Error	Time in sec
No rejection	1.1088	1.8
One threshold	0.0800	1.1
Two thresholds	0.0477	1.7
Worst pairs	0.0488	1.2
Standard deviation	0.0491	1.1

Tab. 2: Results of the different point pair rejection strategies, showing the average registration error and the average computation time.

Obvious from the results in Table 2, is that a rejection strategy is necessary. If no rejection is used the decomposition of matrix *A* in eq. (10) does fail, resulting in a large registration error. The simple rejection strategy with a single threshold works better, but is significantly worse than the more adaptive techniques. The best technique uses two thresholds, but its accuracy is bought dearly considering the average time needed to compute the registration. The best trade off considering time and accuracy is offered by the worst pairs and standard deviation rejection.

Finally, we evaluated the weighting of the point pairs based on their distance and normal compatibility [13]. In our case no improvement considering convergence speed or accuracy could be achieved, probably due to the two step approach and a suitable rejection strategy in place. All in all, we achieved a very good registration result (error ≈ 0.05) in a reasonable amount of time (≈1.1 seconds).

Discussion

We presented a variation of the famous ICP algorithm specifically adapted to the case of registering ear impression surfaces. The proposed algorithm uses a two-step approach. At first, a rough registration is computed using a reduced data representation and the point-to-point error metric. Second, an ICP using the point-to-plane error metric is applied for the final registration.

We evaluated the approach using a sample set containing 400 ear surfaces. The achieved registration results are very good even in case of noise and non-overlapping data (averaged sum of squared distances ≈ 0.05 mm).

In the next steps, we want to utilize the acquired registration information to improve the preprocessing of ear shapes in a CAD system.

Literature

[1] K. S. Arun, T. S. Huang, and S. D. Blostein. “Least-squares fitting of two 3-D point sets”. IEEE Trans. Pattern Anal. Mach. Intell., Vol. 9, No. 5, pp. 698–700, 1987.

[2] P. J. Besl and N. D. McKay. “A Method for Registration of 3-D Shapes”. IEEE Trans. Pattern Anal. Mach. Intell., Vol. 14, No. 2, pp. 239–256, 1992.

[3] I. N. Bronstein and K. A. Semendjajew. Taschenbuch der Mathematik. Thun, Frankfurt am Main: Verlag Harri Deutsch, 5. Auflage Ed., 2001.

[4] Y. Chen and G. Medioni. “Object modelling by registration of multiple range images”. Image Vision Comput., Vol. 10, No. 3, pp. 145–155, 1992.

[5] Henry Gray, “Gray’s anatomy of the human body,” www.bartleby.com/107/, 1918.

[6] M. Kass, A. Witkin, and D. Terzopoulos. “Snakes: Active contour mod- els”. Int. J. of Comp. Vis., Vol. 1, No. 4, pp. 321–331, 1988

[7] R. R. Paulsen, R. Larsen, S. Laugesen, C. Nielsen, and B. K. Ersbøll. “Building and Testing a Statistical Shape Model of the Human Ear Canal”. In: MICCAI 2002, 5th Int. Conference, Tokyo, Japan, Springer, 2002.

[8] S. Rusinkiewicz and M. Levoy. “Efficient Variants of the ICP Algorithm”. In: Proceedings of the Int. Conf. on 3D Digital Imag. and Modeling, pp. 145-152, 2001.

[9] K. Sickel, S. Baloch, V. Bubnik, R. Melkisetoglu, S. Azernikov, T. Fang, and J. Hornegger. “Semi-Automatic Manufacturing of Customized Hearing Aids Using a Feature Driven Rule-based Framework”. In: Proceedings of the VMV Workshop 2009, pp. 305-312, 2009.

[10] Z. Zhang. “Iterative Point Matching for registration of free-form curves”. Tech. Rep., Rapports de Recherche, Programme 4: Robotique, Images et Vision, no. 1658, 1992.

[11] A. Zouhar, T. Fang, G. Unal, and F. McBagonluri. “Anatomically-Aware, Automatic, and Fast Registration of 3D Ear Impression Models”. In: Third Int. Symp. on 3D Data Processing, Visualization, and Transmission, pp. 240 –247, 2006.

Affiliation of the first Author

Konrad Sickel
Pattern Recognition Lab, Department of Computer Science, Friedrich-Alexander-Universität Erlangen-Nürnberg,
Martensstr. 3,
91058 Erlangen,
Germany
Konrad.sickel@informatik.uni-erlangen.de